Asian Journal of Chemistry; Vol. 36, No. 11 (2024), 2659-2665

ASIAN JOURNAL OF CHEMISTRY

https://doi.org/10.14233/ajchem.2024.32686

Preparation of *Tectona grandis* Leaves derived Activated Carbon for High-Performance Supercapacitor Application

C. PRATHEEP[1], K. RAMESH[1,*], M. KIRUTHIGA[2], M. SARAVANAN[1], M. SUGIRTHA[1] and K. SURIDHA[1]

[1]PG and Research Department of Chemistry, Poompuhar College (Affiliated to Bharathidasan University), Melaiyur-609107, India
[2]PG and Research Department of Chemistry, Government College fo Women, Kumbakonam-612001, India

*Corresponding author: E-mail: rameshchemistry944@gmail.com

Received: 9 September 2024; *Accepted*: 24 October 2024; *Published online*: 30 October 2024; AJC-21805

In energy-based applications, biomass porous micro/nanostructures activated carbon materials are the significant candidates, because of their high specific surface area, superior electrical conductivity, affordability and environmental friendliness. In this work, the activated carbon was prepared from *Tectona grandis* leaves as a biomass, and thus activated by 25% K_2CO_3 solution. The prepared carbon was designated as TGLAC. Second carbon was prepared from TGLAC was doped with urea and named as N-doped TGLAC. The physico-chemical analytical methods were employed to access the phase structure, bonding nature and morphological properties of the freshly prepared activated carbon material. Three electrode systems were utilized to estimate the supercapacitor features in 1 M Na_2SO_4 electrolyte. The prepared activated carbon electrode provides a specific capacitance of 371 F g^{-1} at 1 A g^{-1} and a 62% rate capability at 5 A g^{-1}. It retains 94% of its initial capacitance during the cyclic stability analysis at 5 A g^{-1} over 5,000 cycles. This study demonstrates that carbon based materials obtained from sustainable waste biomass can exhibit favourable electrochemical performance in energy applications, providing a clear and feasible synthetic approach and strategy for their utilization.

Keywords: Activated carbon, Energy storage, Supercapacitors, Electrochemistry.

INTRODUCTION

The development of high-performance, safe and effective energy storage systems is essential to sustain human advancement through the utilization of renewable energy technologies [1,2]. To address this issue, various research efforts have been made on the development of supercapacitors for highly efficient energy storage [3]. Due to their rapid discharging and charging processes, extended stability and greater adaptability to harsh conditions than batteries, supercapacitors possess the potential interest [4]. Fundamentally, equipped supercapacitors are emerging as viable electrochemical capacitors with the increasing growth of electric vehicles. Supercapacitors have the potential to offer great power density and rapid response when required. However, one common shortcoming of supercapacitors is their poor energy density. Therefore, scientists work to increase the energy density capacity by creating innovative substances for energy storage and enhancing electrolytes with high operating potential [5,6].

Electrochemical double-layer capacitors (EDLCs) and pseudocapacitors are two types of supercapacitors, which are classified based on the charge storage process depending on how they store energy. While EDLCs preserve charges through reversible ion adsorption at the electrode-electrolyte interface, pseudocapacitors preserve charges through redox reactions. Activated carbon, carbon nanotubes and graphene are among the carbon-based materials actively participating in EDLCs. The conductive polymers and metal oxides can be used as pseudocapacitor electrode materials [7]. The specific capacitance of pseudocapacitive materials is frequently higher than that of EDLC electrodes. Nonetheless, materials based on carbon often possess superior cycle stability and rate capacity. As a result, high-performance materials have been the main focus of the hunt for improved electrode materials for supercapacitors [8]. To achieve outstanding efficiency, it is crucial to design electrode materials that consider factors such as surface morphology, specific surface area, and the degree of graphitization.

Carbon-based materials have drawn a lot of interest among the various energy storage materials used because of their large outer specific surface area, hierarchical porous nature and strong structural stability. Consequently, supercapacitors have a long lifespan, high specific capacitance and high charge/discharge rates. Researchers have created 0D to 3D nanostructured carbon materials with performance for supercapacitor electrodes. Popular carbon compounds like graphene or carbon nanotubes have competitive chemical performance and superior structure. Despite this successful application, energy storage materials continue to face numerous issues. For example, the chemical vapour deposition method used to typically synthesize graphene from fossil fuels faces challenges related to sustainability and environmental degradation. Renewable crops and animals are examples of biomass, which is considered an environmentally beneficial precursor that contributes less pollutants to the nature. Among the materials for energy storage, biomass with inherent organizational assemblies as a starting material could be a viable substitute [9]. A lot of study has also been done recently on the manufacture of electrodes from highly renewable biomass.

Based on the distinctive physico-chemical qualities, such as high electrical conductivity, broad surface area, low cost, superior corrosion resistance and thermal stability, a range of carbon substances have now been selected as supercapacitor electrode materials. Moreover, biomass may be readily transformed into conductive carbon, which is an inexpensive and effective method of recycling biomass. Large-scale uses of some carbon compounds, such as graphene and carbon nanotubes (CNTs), are severely limited by their high-cost need for complex production procedures and scarce raw ingredients, even though high capacitance has been attained with these materials [10]. Consequently, the preparation of low-cost activated carbon-based materials with high conductivity is significant to alternate the commercial materials. Still, various activated carbon materials were prepared by different biomass and thus used for high-performance supercapacitor applications. For example, the activated carbon from biomass was produced from willow catkins using the KOH chemical activation process following the calcination process. This activation carbon provides a specific surface area of 645 $m^2 g^{-1}$ and delivers a 340 F g^{-1} of specific capacitance at 1 A g^{-1} with good cycling stability [11]. Additionally, rice husk was utilized to produce activated carbon by employing three distinct calcination temperatures. It provides a specific surface area of 2696 $m^2 g^{-1}$ and reveals outstanding electrochemical properties, including a specific capacitance of 147 F g^{-1} [12]. The waste tea was used to prepare activated carbon using a chemical activation process encompassing treatment with either K_2CO_3 or H_3PO_4. It exhibits a specific surface area of 1327 $m^2 g^{-1}$ and demonstrates the 203 F g^{-1} of specific capacitance at 1.5 mA cm^{-1} of current density [13]. The pinecone-derived activated carbon delivers the specific capacitance of 185 F g^{-1} in 1 M H_2SO_4 electrolyte [14]. The other works demonstrated the preparation of activated carbon materials from various biomass such as sunflower stalk [15] banana stem, corn-cob and potato starch [10], sugar, rice husk and jute [16], *Acacia auriculiformis* tree [17], cabbage leaves [18], willow wood [19] and aloe vera [20], which were employed as the active electrode materials for supercapacitor application.

This study demonstrates the preparation of activated carbon from *Tectona grandis* leaf biomass for the application in supercapacitors. The biomass was converted into activated carbon using K_2CO_3, followed by calcination at two different temperatures. The physico-chemical analysis confirmed various characterization techniques such as X-ray diffraction (XRD), Fourier transform infrared (FTIR) spectroscopic and scanning electron microscopic (SEM) analysis. The electrochemical analysis was done using cyclic voltammetric (CV) analysis and galvanostatic charge/discharge analysis in three electrode configurations. The electrochemical studies reveal that the prepared activated carbon electrodes deliver high specific capacitance with excellent cyclic stability in 1 M Na_2SO_4 electrolyte. The results additionally revealed that the prepared activated carbons represent potentially useful electrode substances in the applications fields of energy storage.

EXPERIMENTAL

Leaves of *Tectona grandis* were collected from the local garden at Mayiladuthurai district (11.1013º N, 79.6501º E), India. The N-methyl-2-pyrrolidone (NMP), potassium hydroxide (KOH) and sodium sulfate (Na_2SO_4) were procured from SRL (India), while Alfa Aeser was the source of polyvinyl alcohol (PVA, molecular weight 88,000 to 97,000). The Baoji Along with Filtration Material S&T Co., Ltd. China, provides nickel foam.

Synthesis of activated carbon: Initially, 25 g of *T. grandis* leaves were mixed with 25% K_2CO_3 solution. The resultant slurry was left undisturbed at room temperature for 24 h, allowing K_2CO_3 to fully react with the *T. grandis* leaves. After the sample had dried well, it was carbonized in a tubular furnace by heating it in a silica crucible for 2 h at two distinct temperatures (300 ºC and 500 ºC), while being exposed to an N_2 environment. After carbonization, 0.5 M HCl was used to wash the samples, followed by hot distilled water and then cold distilled water until the solution become netural (pH = 7). For doping nitrogen into the activated carbon, urea and carbon (after eliminating acid content) were taken in a 4:1 ratio in a mortar and ground well with 10 mL of deionized water. The obtained blend was heated at 80 ºC for 1 h. Then, the mixture was filtered and dried at 100 ºC for 1 h. Subsequently, the calcination process was conducted according to the activated carbon synthesis procedure. The resulting powder was referred to as nitrogen-doped activated carbon. The resultant plain activated carbon and N-doped activated carbon materials were referred to as TGLAC and N-doped TGLAC, respectively.

Characterization: The powder XRD patterns were recorded using a D8 advαance diffractometer with Cu*K*α radiation (λ = 1.5418 Å) operating at 15 mA, 40 kV, whereas a Perkin-Elmer FTIR spectrometer was used to assess the functional groups in activated carbon. Using a 10 kV accelerating voltage, field emission scanning electron microscopy (FESEM) pictures were recorded using a JEOL JSM-7001F microscope. To test the activated materials' capacitance, a three-electrode setup was used on a CHI 660C electrochemical workstation (Shanghai

ChenHua Instruments Co., China). A 1 M Na_2SO_4 aqueous electrolyte was used for the electrochemical analysis. The active electrode material (90 wt.%) was combined with acetylene black (5 wt.%) and PTFE (5 wt.%) in ultrapure water to prepare the working electrode. The excess water was then removed from the solvent by evaporating it. Using a spatula, the obtained mixture was painted on nickel foam (~1.2 cm^2) and pressed for 10 min at an 8 MPa pressure. Following a 24 h drying process at 80 ºC, the functional electrode was built and comprised approximately 2.0-3.0 mg of activated carbon material. The resultant working electrode was stored for further electrochemical studies.

RESULTS AND DISCUSSION

XRD studies: The phase structure and crystallographic information of TGLAC and N-doped TGLAC carbon materials were studied using XRD analytical method. Fig. 1a shows the XRD result of TGLAC material, which shows the broad peak. This broad peak appears in the 2θ values ranging from 22 to 30º. This broad peak in the XRD spectrum signifies the existence of carbon within the TGLAC material. A confirmation of the formation of pure activated carbon is provided by the absence of any further peaks. Fig. 1b exhibits the XRD pattern of N-doped TGLAC material and the appearance of the two peaks in the XRD pattern is noticeable. The (002) plane of carbon is responsible for the peak at 25º, while the (100) plane of activated carbon is responsible for the high at 43º. These two peaks that remain are typical of activated carbon [21]. The crystalline graphitic structure of carbon is responsible for the extra peaks observed above 40º. The residual peaks that appeared between 30º to 40º are due to the breaking of primary carbon bonds [22]. From TGLAC to N-doped TGLAC activated carbon materials, the XRD pattern intensities rise, suggesting that raising the calcination temperature will enhance the crystalline feature of the activated carbon materials.

FTIR spectral studies: The bonding nature and functional groups of TGLAC and N-doped TGLAC materials were evaluated using FTIR spectroscopy as shown in Fig. 2a-b. The strong and broad peak at 3464 cm^{-1} is linked to the O–H group bands because of the vibrations of the water molecules [23]. The existence of an aliphatic C–H stretch comprising CH, CH_2 and CH_3 groups is reliable for the conspicuous peak at 2924 cm^{-1}. The CH_2 symmetric stretching is attributed to the peak at 2854 cm^{-1}. The existence of C=C groups is the cause of the peak that is observed at 2345 cm^{-1} [24]. The C=N stretching exhibits a peak at 2085 cm^{-1}, while the peak at 1622 cm^{-1} is attributable to C=O stretching in carboxylic acids. The C-H bending vibrations are symmetrical and asymmetric at 1444 cm^{-1}, and the presence of the C-O group in the material may explain the weak band between 900 and 1300 cm^{-1}. The bands appear in 900-500 cm^{-1} region are due to the C–H out-of-plane band's stretching vibrations [25,26].

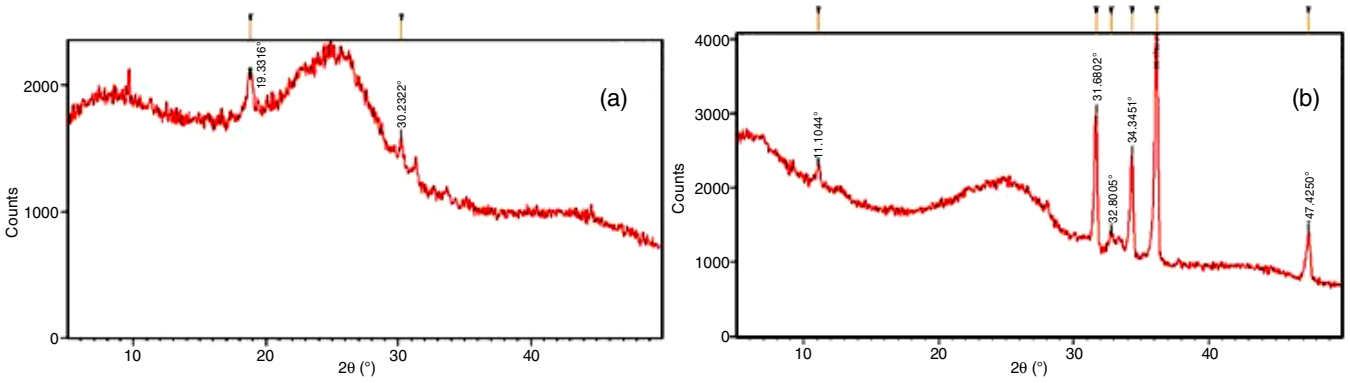

Fig. 1. XRD patterns of (a) TGLAC and (b) N-doped TGLAC material

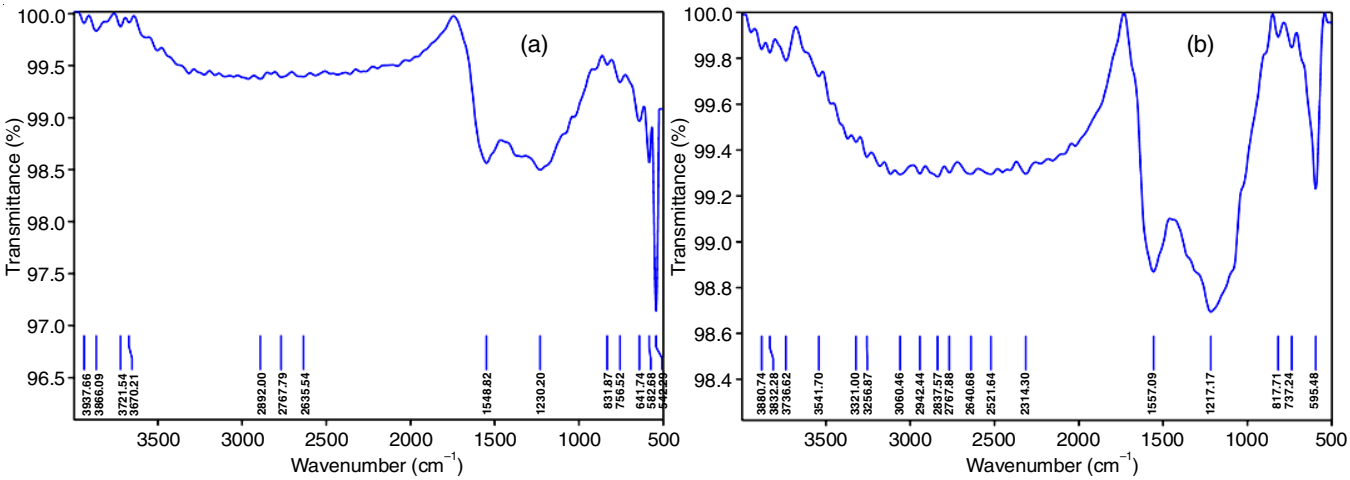

Fig. 2. FTIR spectra of (a) TGLAC and (b) N-doped TGLAC material

Morphological studies: The morphological characteristics of TGLAC and N-doped TGLAC materials were analyzed using SEM analysis. Fig. 3a-b shows the lower and higher magnification SEM images of TGLAC material. SEM pictures showed that the activated carbon's outside surface was incredibly uneven and filled with many voids of varying sizes and shapes. This may occur as a result of the volatile stuff that is created during the activation process gasifying and releasing.

Electrochemical studies: The electrochemical supercapacitor behaviours of obtained TGLAC and N-doped TGLAC samples were initially investigated utilizing a three-electrode electrochemical cell in 1 M Na_2SO_4 electrolyte solution as shown in Fig. 4a-b. The potential limits from -1 to 0 V and a sweep rate from 5 to 100 mV s^{-1} were used for the CV analysis. To activate the material in the electrode, the electrodes were subjected to 50 constant CV tests at a sweep rate of 50 mV s^{-1} before the CV analysis. The electrodes display a quasi-rectangular profile on CV curves, which is a characteristic behaviour associated with EDLC nature [27]. The porous morphology also appeared in N-doped TGLAC material as shown in Fig. 3c-d. The size of the materials is reduced in N-doped TGLAC material when compared to TGLAC material due to the heating process.

Additionally, no discernible redox sign was seen for any of the CV curves, representing that EDLC capacitance is the primary charge storage mechanism in the produced activated carbon samples and that pseudocapacitance is absent from them. Since the oxygen functional groups are generally involved in

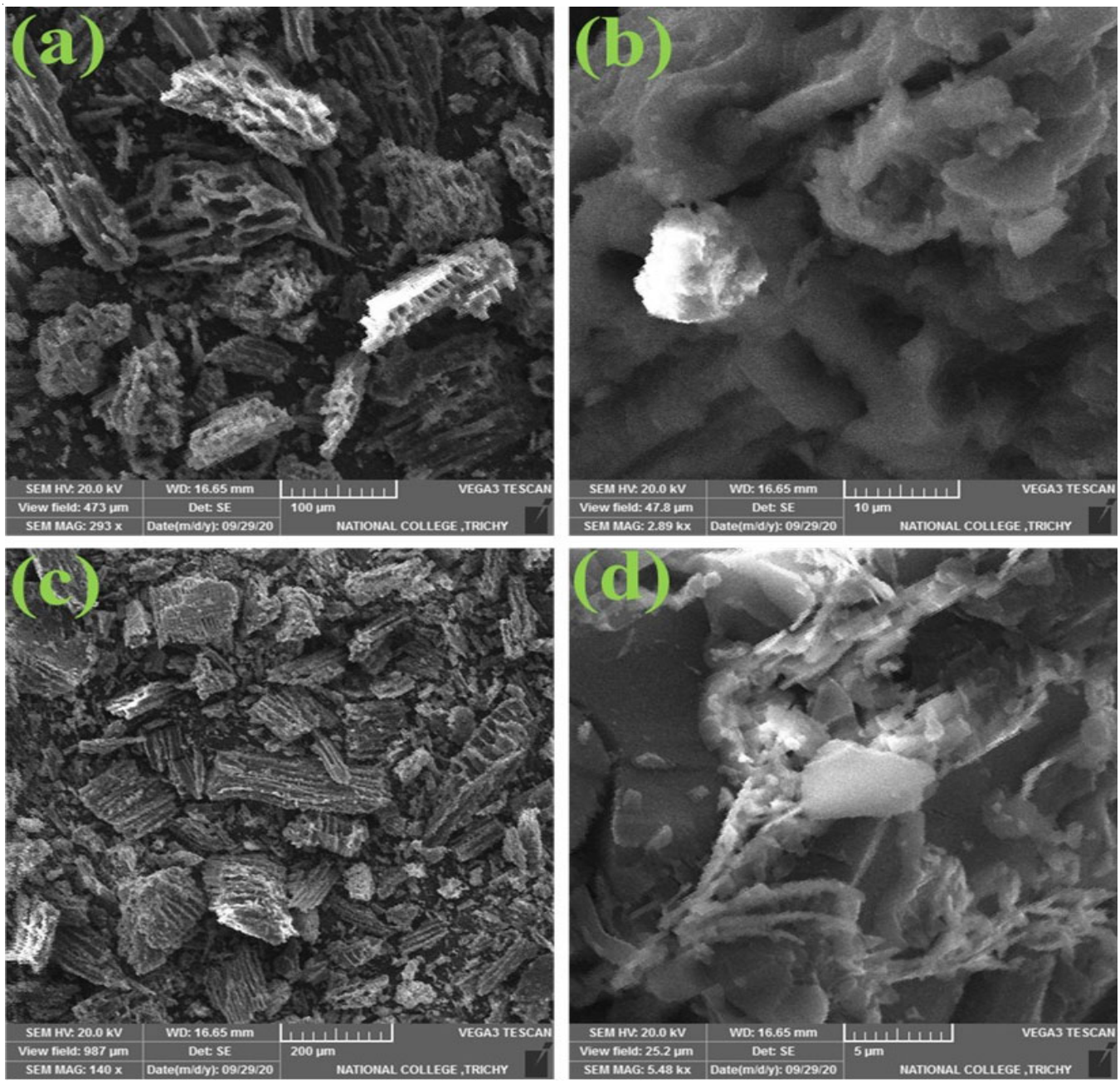

Fig. 3. Lower and higher magnification SEM analysis of (a) & (b) TGLAC and (c) & (d) N-doped TGLAC materials

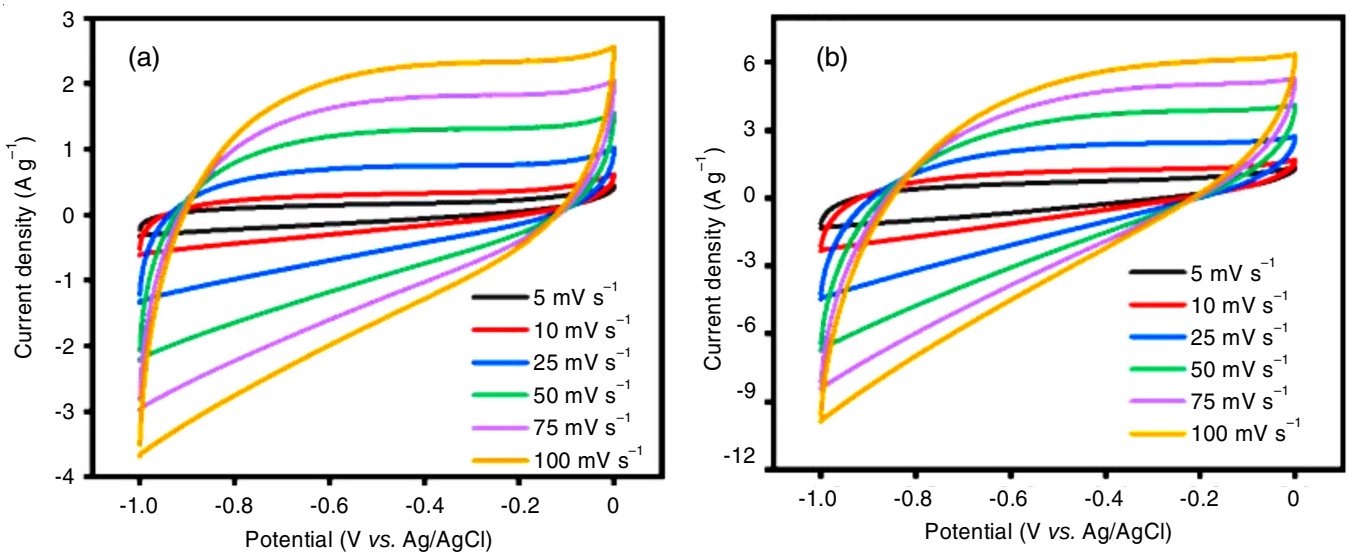

Fig. 4. CV curves of (a) TGLAC and (b) N-doped TGLAC electrodes at various scan rates

faradaic reactions, the lack of pseudocapacitance in activated carbon may be described by the minor presence of these groups within the structure of the material [28]. Even at high sweep rates, all of the CV curves have symmetric rectangular forms, which contain many advantageous characteristics, including a rapid ion diffusion process within the pores, reduced contact or connection resistance, effective charge propagation and speedy rearrangement of the electrical double layer at the switching potentials. These features point to the perfect capacitor behaviour, in which the electrode may quickly accept and release charges while continuing to function even in situations involving rapid cycling [29]. It is clear that the unique capacitance behaviour of material is caused by the area below the CV profile. Interestingly, the N-doped TGLAC electrode exhibits a significant area under the CV curve, suggesting the high supercapacitor characteristics.

The GCD tests were recorded at various current densities to determine the practicality of the prepared electrodes using freshly prepared activated carbon. These tests are essential for evaluating how well the electrode performs in terms of efficiently storing and delivering energy under various charging and discharging circumstances. Important features of supercapacitors can be revealed by the variation of current densities. The GCD curves of TGLAC and N-doped TGLAC electrodes are displayed in Fig. 5a-b, respectively. An internal resistance (iR) reduction was seen in all of the activated carbon electrodes, indicating high conductivity. Furthermore, the symmetric charging and discharging curves of the activated carbon electrodes suggest that the electrodes have strong reversibility [12]. The values of specific capacitance were derived from the discharge time of GCD curves. The specific capacitance of all the GCD curves was calculated using eqn. 1:

$$\text{Specific capacitance} = \frac{I \times \Delta t}{m \times \Delta V} \quad (1)$$

where I is the input current density, Δt is the discharge time, m relates to active material weight and ΔV represents the current density (A g^{-1}), respectively.

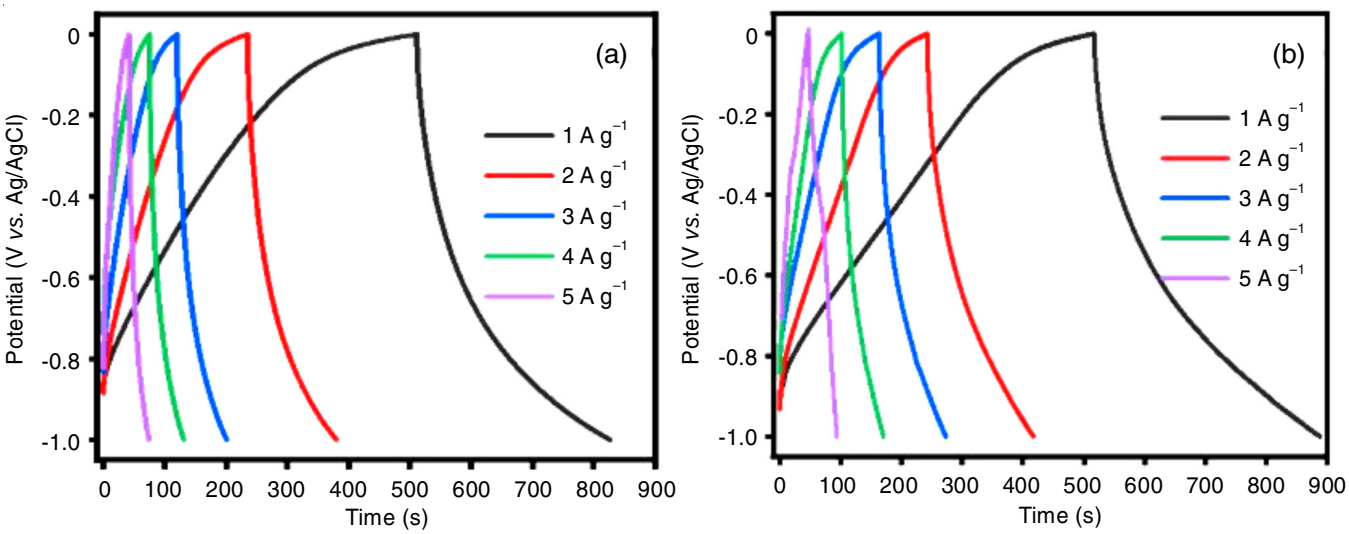

Fig. 5. GCD curves of (a) TGLAC and (b) N-doped TGLAC electrodes at various input current densities

The TGLAC and N-doped TGLAC electrodes deliver the specific capacitance of 316 and 371 F g^{-1}, respectively at 1 A g^{-1} of current density. Among the electrodes, the N-DOPED TGLAC electrode renders a high specific capacitance and thus superior specific capacitance when compared to previous literature based on activated carbon derived from the biomass as shown in Table-1.

TABLE-1
PERFORMANCE COMPARISON TABLE

Activated carbon from the biomass	Electrolyte	Specific capacitance (F g^{-1})	Ref.
Rice husk	6 M KOH	165	[12]
Pistachio shell	1 M KCl	118	[30]
Tectona grandis leaf	1 M H_2SO_4	168	[31]
Tree bark	1 M Na_2SO_4	191	[32]
Anarcadium occidentale	1 M Na_2SO_4	197	[33]
Willow catkins	6 M KOH	340	[11]
Peanut shells	3 M KCl	247	[34]
Leaves of *Tectona grandis*	1 M Na_2SO_4	371	This work

The rate capability property of the prepared electrode was estimated employing the specific capacitance *vs*. current density graph, as shown in Fig. 6. The N-doped TGLAC electrode provides a 62% rate capability at 5 A g^{-1}, which is reasonably better than the TGLAC material (52%) at 5 A g^{-1} of current density value. As current density rises, the specific capacitance marginally falls, which is explained as follows: At low input current density values, the longer operation time allows electrolyte ions to penetrate both the inner area and outer surface regions of the electrode material, leading to maximum utilization of the electrode and, consequently, improved specific capacitance. Conversely, at higher input current densitiy values, the shorter operation time limits the electrochemical process to the outer region of the electrode material, reducing the specific capacitance.

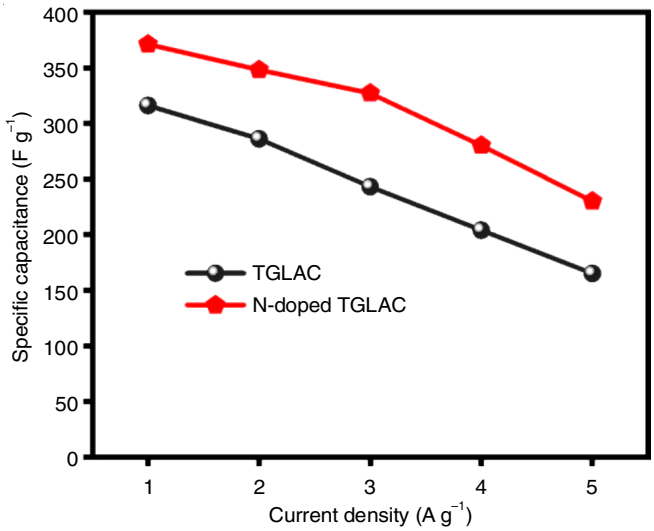

Fig. 6. Specific capacitance *vs*. current density graph

The cyclic stability test was carried out using the GCD test at 5 A g^{-1} for constant 5000 cycles, as shown in Fig. 7. The TGLAC and N-doped TGLAC electrodes exhibit better cyclic stability of 91% and 94% after 5000 cycles. The N-doped TGLAC electrode exhibits high cyclic stability when compared to the TGLAC electrode. Comparatively, the N-doped TGLAC electrode delivers superior electrochemical properties such as specific capacitance, rate capability and cyclic stability than the TGLAC electrode.

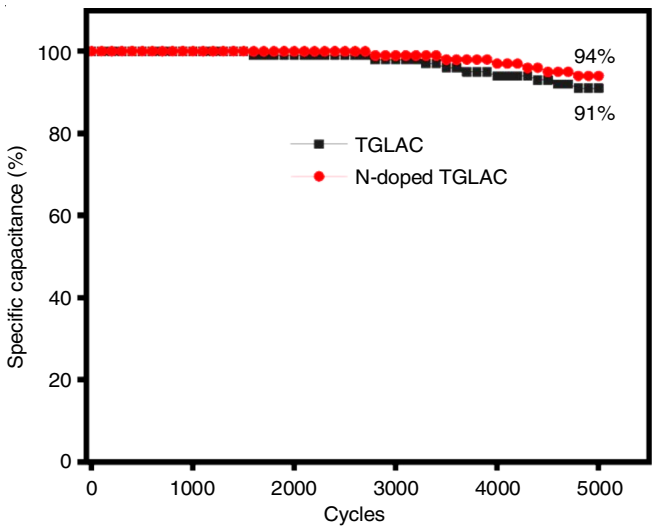

Fig. 7. Cyclic stability analysis at 5 A g^{-1} for 5000 GCD cycles

Conclusion

This study presents a potential approach to effectively and optimally utilize sustainable waste biomass resources for the production of highly active carbons as electrode materials in high-performance energy storage and conversion devices. The *Tectona grandis* leaves were employed to produce the activated carbon using 25% K_2CO_3 solution. The newly prepared activated carbon material's phase structure, bonding type and morphological characteristics were assessed using physico-chemical analytical techniques. In 1 M Na_2SO_4 electrolyte, three-electrode electrochemical configurations were used to assess the supercapacitor's performance. A specific capacitance of 371 F g^{-1} at 1 A g^{-1} of input current density and an exceptional rate capability of 62% at 5 A g^{-1} are provided by the prepared N-doped TGLAC activated carbon electrode. After 5,000 GCD cycles at 5 A g^{-1} of current density, it can sustain 94% of its initial capacitance.

CONFLICT OF INTEREST

The authors declare that there is no conflict of interests regarding the publication of this article.

REFERENCES

1. F.W. Richey, C. Tran, V. Kalra and Y.A. Elabd, *J. Phys. Chem. C*, **118**, 21846 (2014); https://doi.org/10.1021/jp506903m
2. Q. Geng, H. Wang, J. Wang, J. Hong, W. Sun, Y. Wu and Y. Wang, *Small Methods*, **6**, 2200314 (2022); https://doi.org/10.1002/smtd.202200314
3. Q. Chen, X. Tan, Y. Liu, S. Liu, M. Li, Y. Gu, P. Zhang, S. Ye, Z. Yang and Y. Yang, *J. Mater. Chem. A Mater. Energy Sustain.*, **8**, 5773 (2020); https://doi.org/10.1039/C9TA11618D
4. Z. Wang, D. Shen, C. Wu and S. Gu, *Green Chem.*, **20**, 5031 (2018); https://doi.org/10.1039/C8GC01748D

5. Q. Wang, J. Yan and Z. Fan, *Energy Environ. Sci.*, **9**, 729 (2016); https://doi.org/10.1039/C5EE03109E
6. V. Strauss, K. Marsh, M.D. Kowal, M. El-Kady and R.B. Kaner, *Adv. Mater.*, **30**, 1704449 (2018); https://doi.org/10.1002/adma.201704449
7. J. Wang, X. Zhang, Z. Li, Y. Ma and L. Ma, *J. Power Sources*, **451**, 227794 (2020); https://doi.org/10.1016/j.jpowsour.2020.227794
8. F. Abnisa and W.M.A. Wan Daud, *Energy Convers. Manage.*, **87**, 71 (2014); https://doi.org/10.1016/j.enconman.2014.07.007
9. G. Emilsson, E. Röder, B. Malekian, K. Xiong, J. Manzi, F.-C. Tsai, N.-J. Cho, M. Bally and A. Dahlin, *Front Chem.*, **7**, 1 (2019); https://doi.org/10.3389/fchem.2019.00001
10. H. Meskher, D. Ghernaout, A.K. Thakur, F.S. Jazi, Q.F. Alsalhy, S.S. Christopher, R. Sathyamurhty and R. Saidur, *Mater. Today Commun.*, **38**, 108517 (2024); https://doi.org/10.1016/j.mtcomm.2024.108517
11. K. Wang, N. Zhao, S. Lei, R. Yan, X. Tian, J. Wang, Y. Song, D. Xu, Q. Guo and L. Liu, *Electrochim. Acta*, **166**, 1 (2015); https://doi.org/10.1016/j.electacta.2015.03.048
12. E.Y.L. Teo, L. Muniandy, E.P. Ng, F. Adam, A.R. Mohamed, R. Jose and K.F. Chong, *Electrochim. Acta*, **192**, 110 (2016); https://doi.org/10.1016/j.electacta.2016.01.140
13. I.I.G. Inal, S.M. Holmes, A. Banford and Z. Aktas, *Appl. Surf. Sci.*, **357**, 696 (2015); https://doi.org/10.1016/j.apsusc.2015.09.067
14. M. Rajesh, R. Manikandan, S. Park, B.C. Kim, W.J. Cho, K.H. Yu and C.J. Raj, *Int. J. Energy Res.*, **44**, 8591 (2020); https://doi.org/10.1002/er.5548
15. X. Wang, S. Yun, W. Fang, C. Zhang, X. Liang, Z. Lei and Z. Liu, *ACS Sustain. Chem. Eng.*, **6**, 11397 (2018); https://doi.org/10.1021/acssuschemeng.8b01334
16. K. Ojha, B. Kumar and A.K. Ganguli, *J. Chem. Sci.*, **129**, 397 (2017); https://doi.org/10.1007/s12039-017-1248-8
17. M. Jalalah, S. Rudra, B. Aljafari, M. Irfan, S.S. Almasabi, T. Alsuwian, M.I. Khazi, A.K. Nayak and F.A. Harraz, *Electrochim. Acta*, **414**, 140205 (2022); https://doi.org/10.1016/j.electacta.2022.140205
18. P. Wang, Q. Wang, G. Zhang, H. Jiao, X. Deng and L. Liu, *J. Solid State Electrochem.*, **20**, 319 (2016); https://doi.org/10.1007/s10008-015-3042-1
19. J. Phiri, J. Dou, T. Vuorinen, P.A.C. Gane and T.C. Maloney, *ACS Omega*, **4**, 18108 (2019); https://doi.org/10.1021/acsomega.9b01977
20. M. Karnan, K. Subramani, N. Sudhan, N. Ilayaraja and M. Sathish, *ACS Appl. Mater. Interfaces*, **8**, 35191 (2016); https://doi.org/10.1021/acsami.6b10704
21. Z. Xu, T. Zhang, Z. Yuan, D. Zhang, Z. Sun, Y.X. Huang, W. Chen, D. Tian, H. Deng and Y. Zhou, *RSC Adv.*, **8**, 38081 (2018); https://doi.org/10.1039/C8RA06253F
22. S.K. Shahcheragh, M.M. Bagheri Mohagheghi and A. Shirpay, *SN Appl. Sci.*, **5**, 313 (2023); https://doi.org/10.1007/s42452-023-05559-6
23. T.A. Saleh and G.I. Danmaliki, *J. Taiwan Inst. Chem. Eng.*, **60**, 460 (2016); https://doi.org/10.1016/j.jtice.2015.11.008
24. M. Baikousi, K. Dimos, A.B. Bourlinos, R. Zboøil, Y. Deligiannakis, I. Papadas and M.A. Karakassides, *Appl. Surf. Sci.*, **258**, 3703 (2012); https://doi.org/10.1016/j.apsusc.2011.12.010
25. M. Veerapandian, N. Lévaray, M.H. Lee, S. Giasson and X.X. Zhu, *ACS Appl. Mater. Interfaces*, **7**, 14552 (2015); https://doi.org/10.1021/acsami.5b00608
26. A.G. Santos, G.O. da Rocha and J.B. de Andrade, *Sci. Rep.*, **9**, 1 (2019); https://doi.org/10.1038/s41598-018-37186-2
27. M.D. Stoller, S. Park, Y. Zhu, J. An and R.S. Ruoff, *Nano Lett.*, **•••**, 6 (2008).
28. N. Zhao, S. Wu, C. He, C. Shi, E. Liu, X. Du and J. Li, *Mater. Lett.*, **87**, 77 (2012); https://doi.org/10.1016/j.matlet.2012.07.085
29. B. Fang and L. Binder, *J. Power Sources*, **163**, 616 (2006); https://doi.org/10.1016/j.jpowsour.2006.09.014
30. Ö. Sahin, Y. Yardim, O. Baytar and C. Saka, *Int. J. Hydrogen Energy*, **45**, 8843 (2020); https://doi.org/10.1016/j.ijhydene.2020.01.128
31. E. Taer, M. Melisa, A. Agustino, R. Taslim, W. Sinta Mustika and A. Apriwandi, *Energy Sources A Recovery Util. Environ. Effects*, **00**, 1 (2021); https://doi.org/10.1080/15567036.2021.1950871
32. D. Momodu, M. Madito, F. Barzegar, A. Bello, A. Khaleed, O. Olaniyan, J. Dangbegnon and N. Manyala, *J. Solid State Electrochem.*, **21**, 859 (2017); https://doi.org/10.1007/s10008-016-3432-z
33. P. Merin, P. Jimmy Joy, M.N. Muralidharan, E. Veena Gopalan and A. Seema, *Chem. Eng. Technol.*, **44**, 844 (2021); https://doi.org/10.1002/ceat.202000450
34. T. Manimekala, R. Sivasubramanian, S. Karthikeyan and G. Dharmalingam, *J. Porous Mater.*, **30**, 289 (2023); https://doi.org/10.1007/s10934-022-01338-7